NUMERICAL SIMULATION OF STRESS DISTRIBUTION FOR TOROIDAL DRIVE

Lizhong Xu Lei Zhang
Mechanical engineering institute, Yanshan University, Qinhuangdao 066004, China
xlz@ysu.edu.cn

Received August 2005, Accepted April 2006
No. 05-CSME-51, E.I.C. Accession 2903

ABSTRACT

In this paper, in the environment of the Pro/Engineer software package, 3D model of the drive is constructed. FEM analysis package, Pro/Engineer, is used to calculate stress distribution in the elements for the toroidal drive under loads. The stress distributions on worm, stator and planet for the drive are obtained. Changes of the stress distribution along with planet rotating angle and planet number are presented. The results show: The load share among the contact tooth pairs is not uniform. The maximum stress in the stator is larger than that in the worm. As planet rotates, stress distribution on the stator and worm changes periodically. At two teeth mesh zone, the maximum stress on the stator or worm is larger than that at three teeth mesh zone. Increase of the planet number can reduce stress in the toroidal drive. It is because uniform stress distribution and more sharing points of the load.

LA SIMULATION NUMERIQUE DE LA DISTRIBUTION DE CONTRAINTE DE LA TRANSMISSION TOROÏDALE

RESUME

Dans cet article, le modèle de 3D de la transmission est réalisé en pratiquant le logiciel de Pro/Engineering. Aussi, le logiciel de l'élément limité de Pro/Engineering est utilisé pour le calcul de distribution de contrainte en pièce de transmission rechargé tels que l'arbre à vis sans fin, le stator et les roues à l'étoile et ainsi que la relation entre la distribution de contrainte et l'angle de rotation, et celle entre la distribution de contrainte et le nombre des roues sont découverts. Il en résulte que le chargement entre les dents de contacts est irrégulier. La contrainte maximale de stator est supérieure à celle d'arbre à vis sans fin. La distribution de contrainte dans le stator et l'arbre à vis sans fin se change d'une manière cyclique avec le fonctionnement des roues à l'étoile. A la zone de contact des deux dents, la contrainte maximale dans le stator et l'arbre à vis sans fin est supérieure à celle de trios dents. L'augmentation de nombre des roues permet de réduire la contrainte dans l'arbre toroïdal à vis sans fin, comme cela se fait par l'augmentation des points chargés et régulières.

1. Introduction

The toroidal drive was proposed by M.R.Kuehnle in1966[1]. The drive consists of four basic elements, Fig.1: (a) the central input worm; (b) radically positioned planets; (c) a stator of toroidal shape; and (d) a rotor, which forms the central output shaft upon which the planets are mounted. The input worm rotates each planet about its own axis. The planets have balls or rollers instead of teeth. Each planet meshes with the toroidal grooves in the stator. The rotor is the output. The drive can transmit large torque in a very small size and is suitable for top end technical fields such as aviation and space flight, etc.

M.R.Kuehnle and H.Peeken invented a special machine tool to produce stator[2]. S.Cerniak et al. proposed a calculation method for the tooth profile of the stator and its machining principle[3]. H.Peeken et al. studied pitting problems on stator surface and the load distributions on stator and worm[4-5]. Tooten presented a method for the determination of the non-uniform distribution of load along the contact line on planet tooth surface[6]. Lizhong Xu investigated mesh theory and contact stress of the toroidal drive[7-8] .

The relative motions between different elements in the drive occur in three dimensional spaces, planet meshes with stator and worm simultaneously in a toroidal path. There are complicated kinematics, geometrics and mechanics relations between conjugate profiles of the drive. Therefore, development of the design theory for the drive is difficult. In operation, pitting is the main type of the failures in toroidal drive. It is the fatigue failure of the tooth surfaces because of many repetitions of high contact stresses. Prolonged operation on a pit surface will cause vibration and noise. Therefore, the calculation of the contact stresses is required. However, the stress distribution and stress field in the main elements for the drive had not been investigated yet before authors. It causes unreliable estimation of load-carrying ability for the drive. In 2003, authors presented analytical equations of the contact stresses for the drive [7]. In paper [7], more factors were neglected for simplifying analysis. In order to obtain more accurate contact stress distribution, a numerical simulation of the contact stresses is required.

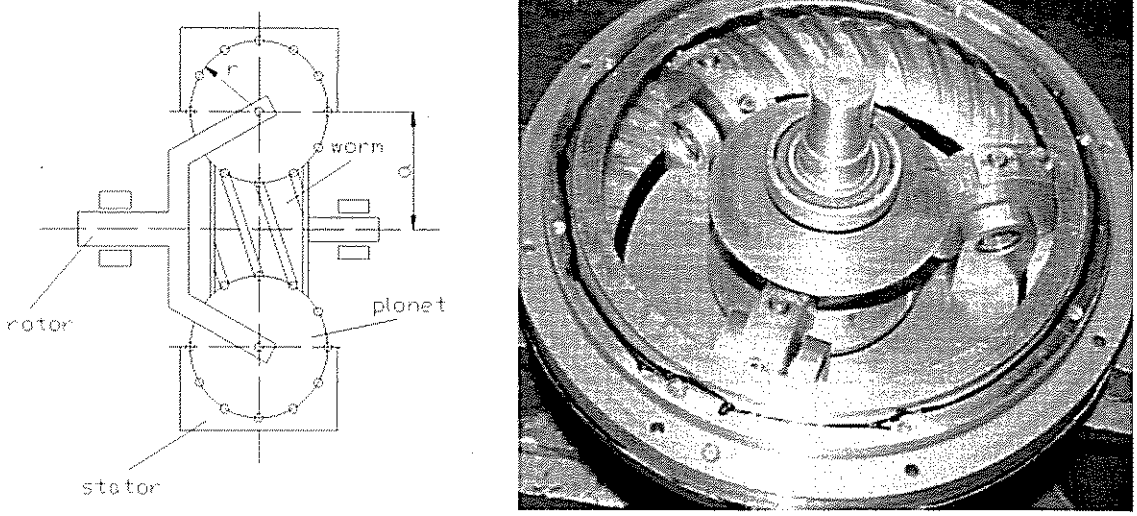

(a) (b)

Fig.1 The toroidal drive
(a) Diagram of the drive (1. Planet 2. Worm 3. Stator 4. Rotor) (b) Model machine of the drive

In this paper, based on center curve of the teeth, in the environment of the Pro/Engineer software package, 3D stator and worm models, and 3D model of the drive are constructed. FEM analysis package, Pro/Engineer, is used to calculate stress distribution in the elements for the toroidal drive under loads. The stress distributions in worm, stator and planet for the drive are obtained. Changes of the stress distribution along with planet rotating angle and planet number are presented. The results show: The load share among the contact tooth pairs is not uniform, near torque input end, the stress in the worm is larger, and near torque output end, the stress in the stator is larger. The maximum stress in the stator is larger than that in the worm. As planet rotates, stress distribution in the stator and worm changes periodically. At two teeth mesh zone, the maximum stress in the stator or worm is larger than those at three teeth mesh zone. Increase of the planet number can reduce stress in the toroidal drive. It is because uniform stress distribution and more sharing points of the load. These results are useful in design and manufacture of the drive. The research can also offer reference for the stress analysis of other drives and structures with toroidal elements.

2. Solid model of the toroidal drive

The teeth of the stator and worm are cut on the toroidal surface of the stator or worm blank, among which the teeth of the stator are cut on the internal toroidal surface, so it is difficult to construct their 3D models. Their basis is calculation of the pattern curves. In planet coordinate system, the center of the planet tooth can be calculated easily. The center of the planet tooth is transformed to stator coordinate system, the center of the stator tooth can be given. The center of the planet tooth is transformed to worm coordinate system, the center of the helical tooth for worm can be given as well. Thus, the pattern curves of the stator and worm teeth are obtained. Based on center curve of the teeth, in the environment of the Pro/Engineer software package, the 3D stator and worm models can be constructed. It is indicated as follows:

(1) Built stator and worm blanks: Based on given design parameters(the main parameters of the drive are shown in Table 1, some main dimensions of the toroidal drive are drawn in an outline sketch. Then, by means of command "Rotate", a solid stator or worm blank is created.

(2) Built a sweep path: By means of command "Insert base curve", and the sweep curve can be created from tooth center equations.

(3) A single stator or worm tooth: The tooth cross section of the stator and worm is taken as trapezoid perpendicular to center curve of the stator tooth. Applying a command "helical sweep" in the environment of the Pro/Engineer software package and going through above trapezoid cross section, a single stator and worm helix tooth is created.

(4) The whole stator or worm model: Applying a command "Pattern", above single stator or worm tooth is patterned into several teeth arrayed evenly and radially and the 3D stator or worm model is constructed as shown in Fig.2(a) and (b). In the toroidal drive, the worm is supported on bearings which are mounted at the two ends of the worm. In Fig.2(b), the total worm shaft is shown. And in Fig.1(a), as a diagram of the drive, the part of the shaft on left of the worm is neglected.

(5) Construction of the 3D planet model does not involve curve pattern and can be created easily as shown in Fig.2(c).

(6) In the environment of the Pro/Engineer software package, several "Assembly" commands are given, and above stator, worm, and planets are placed and assembled

together with rotor and the solid model for the drive is created. The 3D drive model is shown in Fig.2(d).

Table1 The main parameters for the drive

Parameters	data
Center distance a	120mm
Planet tooth number z_1	8
Worm thread number z_2	1
Stator tooth number z	35
Planet radius R	62.5mm
Face width angle of the worm ϕ_v'	100^0
Face width angle of the stator ϕ_v	120^0
Half cone angle of the planet tooth δ	10^0

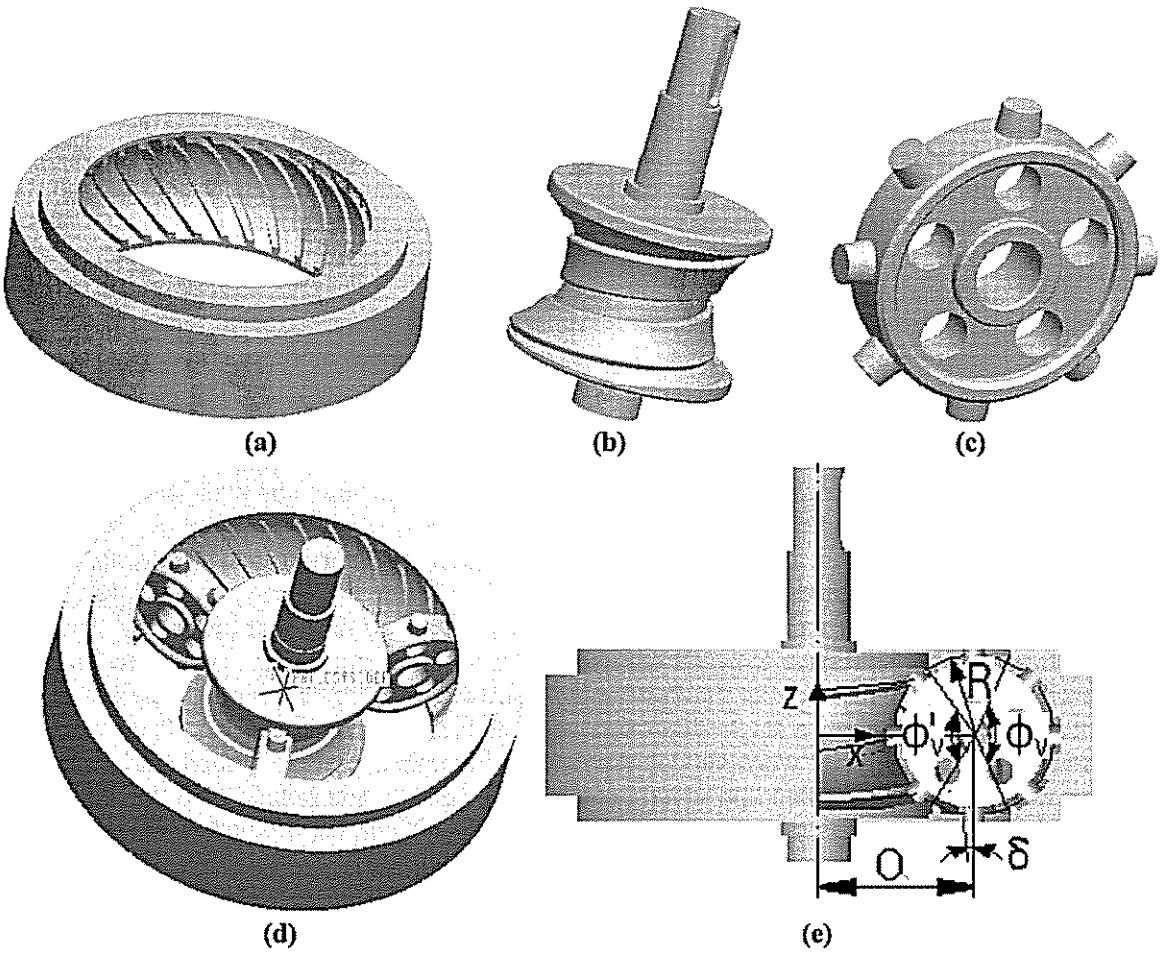

Fig.2 3D models of the drive and main elements
(a) 3D stator model (b) 3D worm model (c) 3D planet model (d) 3D models of the drive (e) the main parameters of the drive

3. FEM model and Mesh division

In this investigation, FEM analysis package, Pro/Engineer, is used to calculate stress in the elements for the toroidal drive under loads. Parameters of the example drive system are shown in Table 1. FEM models and mesh-dividing patterns for stress analysis of the drive are shown in Fig.3. Here, p-adaptive remeshing scheme and tetrahedral units are used. In Fig.3, element number of the FEM is 4720, and nodes number is 1706, order number of the interpolation polynomial is seven. Fig.3(a) shows FEM model and initial mesh-dividing pattern of the drive. Fig.3(b),(c) and (d) show FEM models and initial mesh-dividing patterns of the worm, planet and stator, respectively. Here, only one planet is considered. In order to improve calculating accuracy, command "Localized Mesh Refinement" is chosen. So element number of the FEM at contact regions is increased. The mesh-dividing patterns at contact region between planet and worm are shown in Fig.4(a), and the mesh-dividing patterns at contact region between planet and stator in Fig.4(b). Under condition that the convergence accuracy is 10%, the mesh convergence curve is shown in Fig.5. Here, Multi-Pass Adaptive iteration is selected is used to calculate contact stresses between planet and worm or stator. In operation of the drive, the rolling friction occurs between mesh tooth pairs, and full lubrication is assured. Thus, the friction forces between planet teeth and worm or stator are quite small and can be neglected. Therefore, the friction coefficient is taken as zero.

In operation of the toroidal drive, the planet orbit with its own axis and it also along with rotor orbits with fixed axis. For simplifying analysis, the rotor is considered to be fixed, and the stator is considered to rotate about center axis. Thus, the only one rotating freedom degree is remaining for the planet and its boundary condition and load can be given easily. The boundary conditions and loads of the total drive are shown in Fig.6(a). For the stator, three translational and two rotational freedom degrees are removed, only one rotational freedom degree about center axis is remain as shown in Fig.6(a), (f) and (g), here the restraint is applied to outer cylindrical surface of the stator. For the worm, three translational and two rotational freedom degrees are removed, only one rotational freedom degree about center axis is remain as well as shown in Fig.6(a), (b) and (c). For the planet, three translational and two rotational freedom degrees are removed, only one rotational freedom degree about its own axis is remain as shown in Fig.6(a), (d) and (e), here the restraint is applied to inter cylindrical surface of the planet center hole.

An input torque is applied to worm axis, and an output torque is applied to the stator as shown in Fig.6(a), (b), (c), (f) and (g). In Fig.6, T_1 is input torque, T_2 is output torque, $T_2 = T_1 \times i \times \eta$. Here, i is speed ratio of the drive, η is operating efficiency of the drive. Here, stator, worm, planet and rotor are made of steel. In this analysis, Modulus of elasticity of steel is 206Gpa, and Poisson's ratio is 0.3. The operating efficiency of the example drive is given by measurement. The operating efficiency is 92%. And the speed ratio $i = 36$.

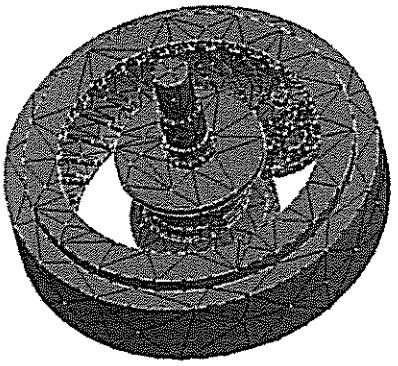

(a)

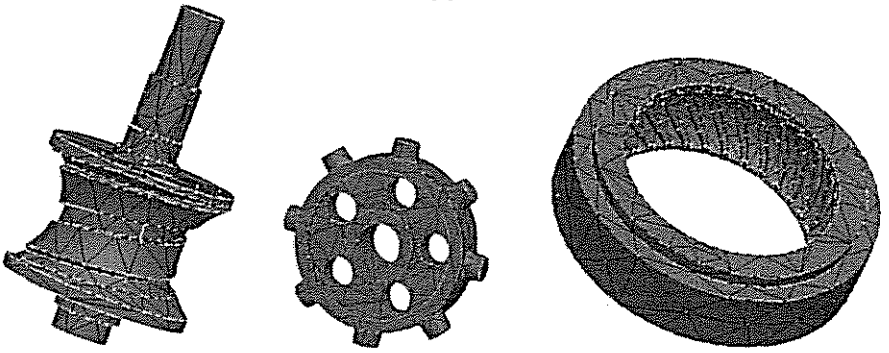

(b) (c) (d)

Fig.3 FEM model and initial mesh division of the drive and main elements
(a) drive (b) worm (c) planet (d) stator

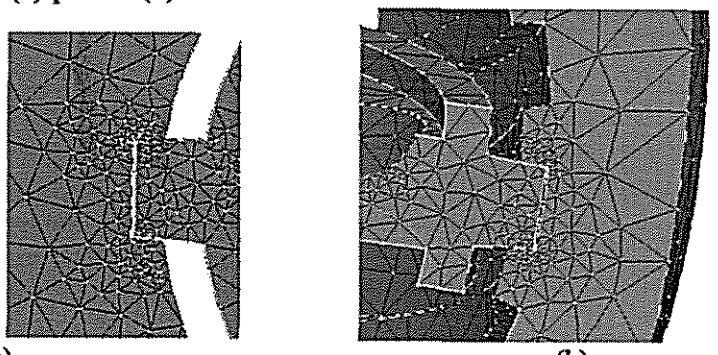

(a) (b)

Fig.4 The mesh-dividing patterns at contact regions
(a) between planet and worm, (b) between planet and stator

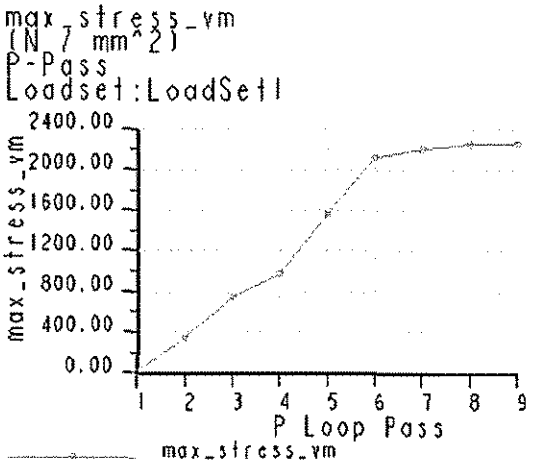

Fig.5 The mesh convergence curve

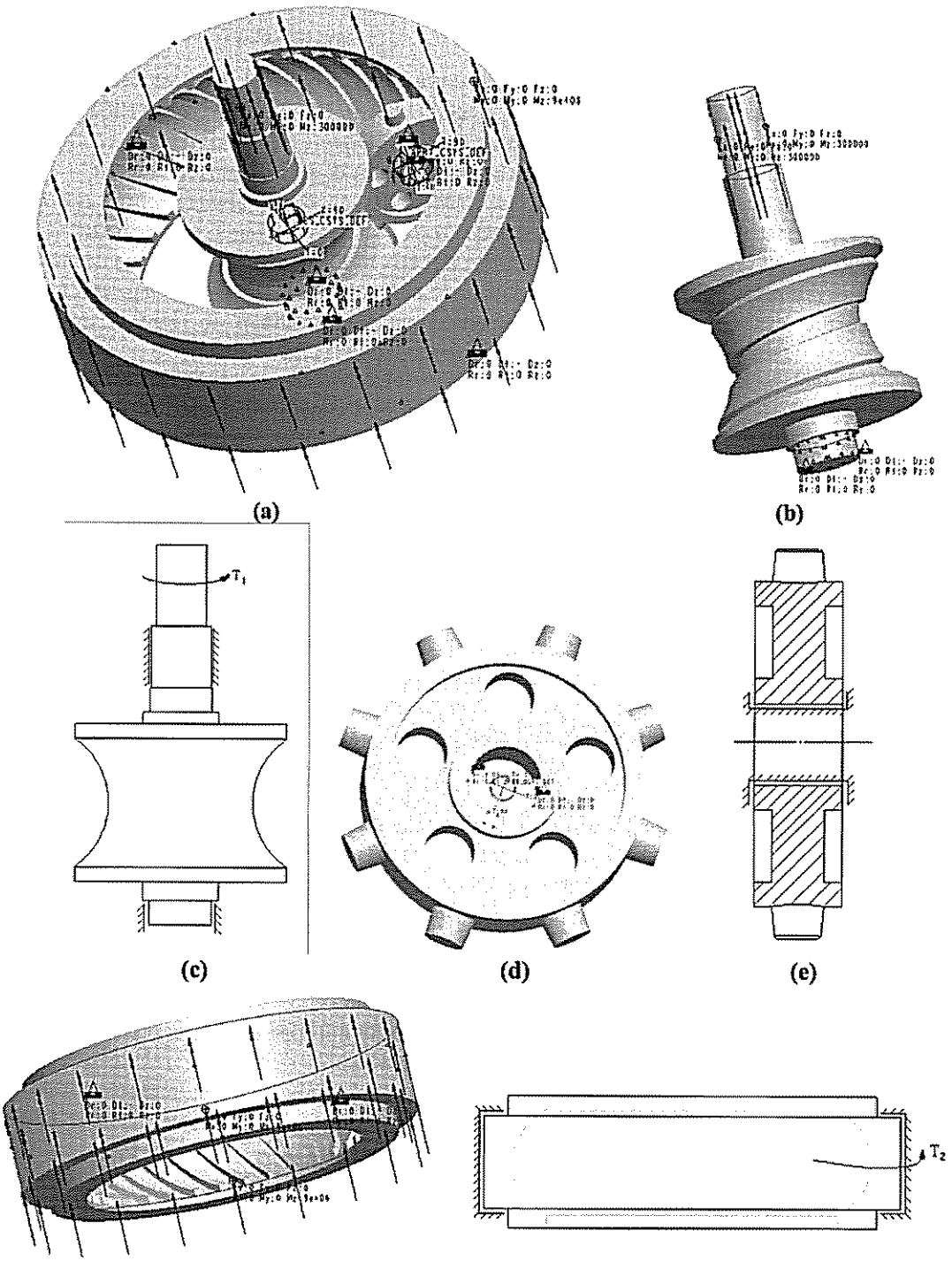

Fig.6 The boundary conditions and loads on FEM model
(a) 3D drive model, (b) 3D worm model, (c) load and boundary condition diagram of worm, (d) 3D planet model, (e) load and boundary condition diagram of planet, (f) 3D stator model, (g) load and boundary condition diagram of stator

4. Stress distribution in the drive

By above FEM model and boundary conditions, the stress distributions in a toroidal drive are presented as shown in Figs.7, 8, and 9 (here T_1=150N.m, T_2=5000N.m). Fig.7 shows the von-Mises stress distribution in the worm. Fig.8 shows von-Mises stress distribution in the stator. Fig.9 shows von-Mises stress distribution in the planet.

In Fig.7, stress distributions of three contact tooth pairs between worm and a planet are shown. Here, window 1 revolves around axis y for -90°. From Fig.7, it is known:

(1) The load share among the contact tooth pairs is not uniform. Near torque input end, the stress is the maximum (1309MPa) as shown in left partial enlarged drawing, and at another end of the worm the stress is the minimum (390MPa) as shown in right partial enlarged drawing. Ratio of the maximum stress to the minimum is 3.3.

(2) For each contact tooth pair, the shape of the contact zone is narrow and long. At the two ends of each contact zone, the stress is larger and dumbbell-shaped stress distribution occurs. It is because non uniform load distribution between mesh teeth of the worm and planet caused by elastic deformation of the planet tooth.

In Fig.8, stress distributions of three contact tooth pairs between stator and a planet are shown. From Fig.8, it is known:

(3) The load share among the contact tooth pairs is not uniform as well. The contact stress at the medium contact point is the maximum (1785MPa) as shown in partial enlarged number 2 drawing. Near torque output end, the stress is larger than that at another end of the stator. The stress near torque output end is 1428MPa as shown in partial enlarged number 3 drawing. The stress near torque input end is 714MPa as shown in partial enlarged number 1 drawing. Ratio of the maximum stress to the minimum is 2.5. So the stress distribution between planet and stator is more uniform than that between planet and worm. Here, larger stress at output end is caused by elastic deformation of the stator and planet.

(4) For each contact tooth pair, just like worm teeth, the shape of the contact zone is narrow and long as well. At the two ends of each contact zone, the stress is larger and dumbbell-shaped stress distribution occurs. It is because the same reason as above.

(5) The maximum stress (1785MPa) in the stator is larger than that (1309MPa) in the worm. This result is in agreement with one of the reference [7].

In Fig.9, stress distributions in the planet are shown. Number 1, 2 and 3 teeth mesh with worm, and number 4, 5 and 6 teeth mesh with the stator. From Fig.9, it is known:

(6) Among number 1, 2 and 3 teeth, the stress on the number 1 tooth is the maximum. It is because the tooth corresponds to input end of the worm.

(7) Among number 4, 5 and 6 teeth, the stress on the number 5 tooth is the maximum. It is because the tooth corresponds to the medium contact point between the planet and stator.

Simulation results show that the maximum contact stress occurs on the tooth surface of the planet. Under T_1=150N.m and T_2=5000N.m, when only one planet is considered, the maximum contact stress on the planet tooth surface is 2338MPa which is larger than yield strength of the planet material. The planet tooth is made of 40CrNiMo, yield strength of which is 835 MPa. It shows that three planets should be used to carrying aforementioned loads.

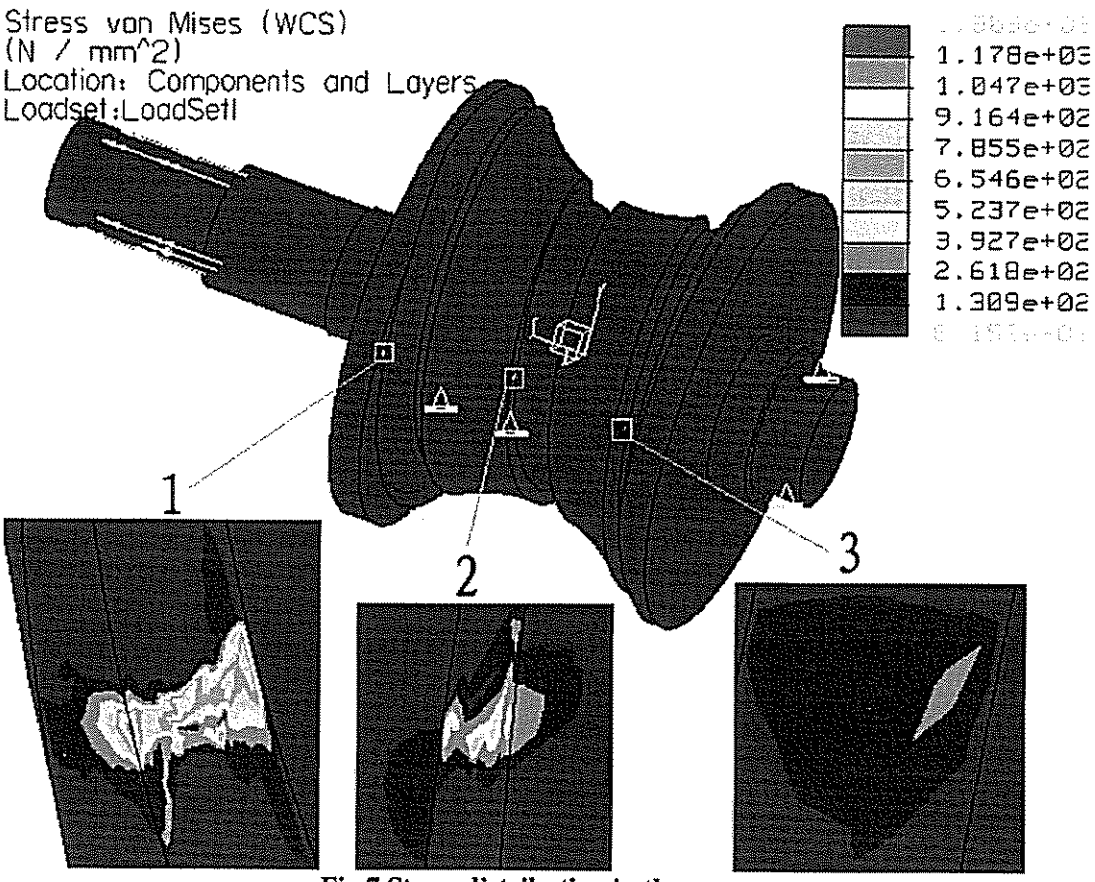

Fig.7 Stress distribution in the worm

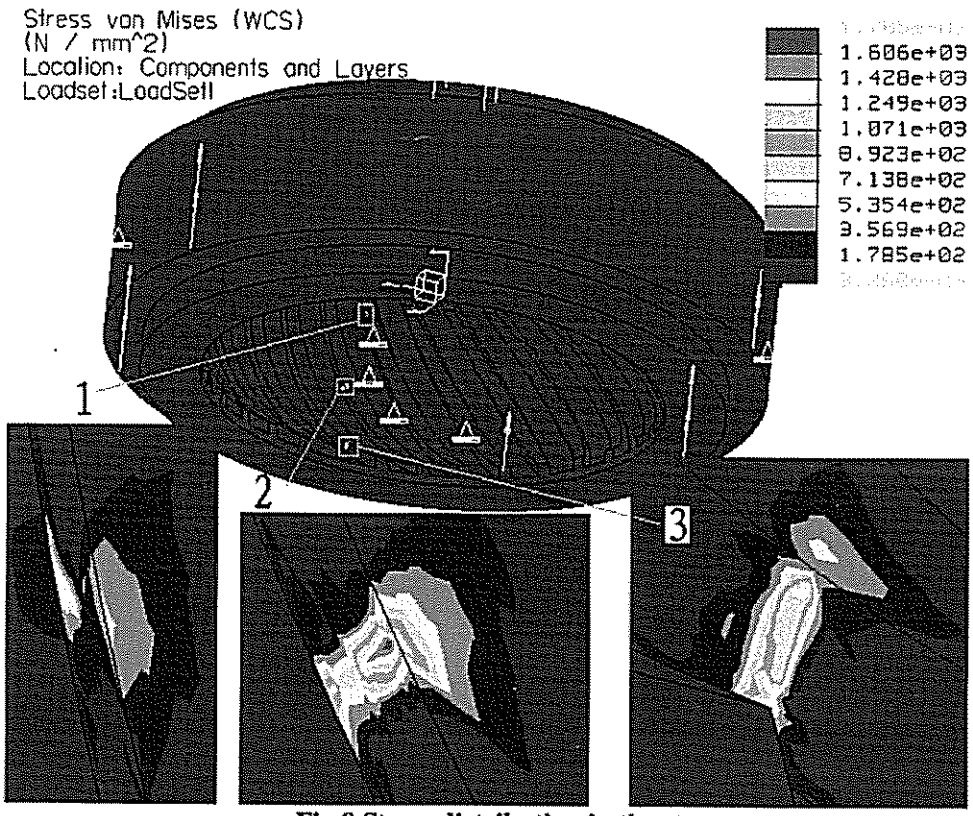

Fig.8 Stress distribution in the stator

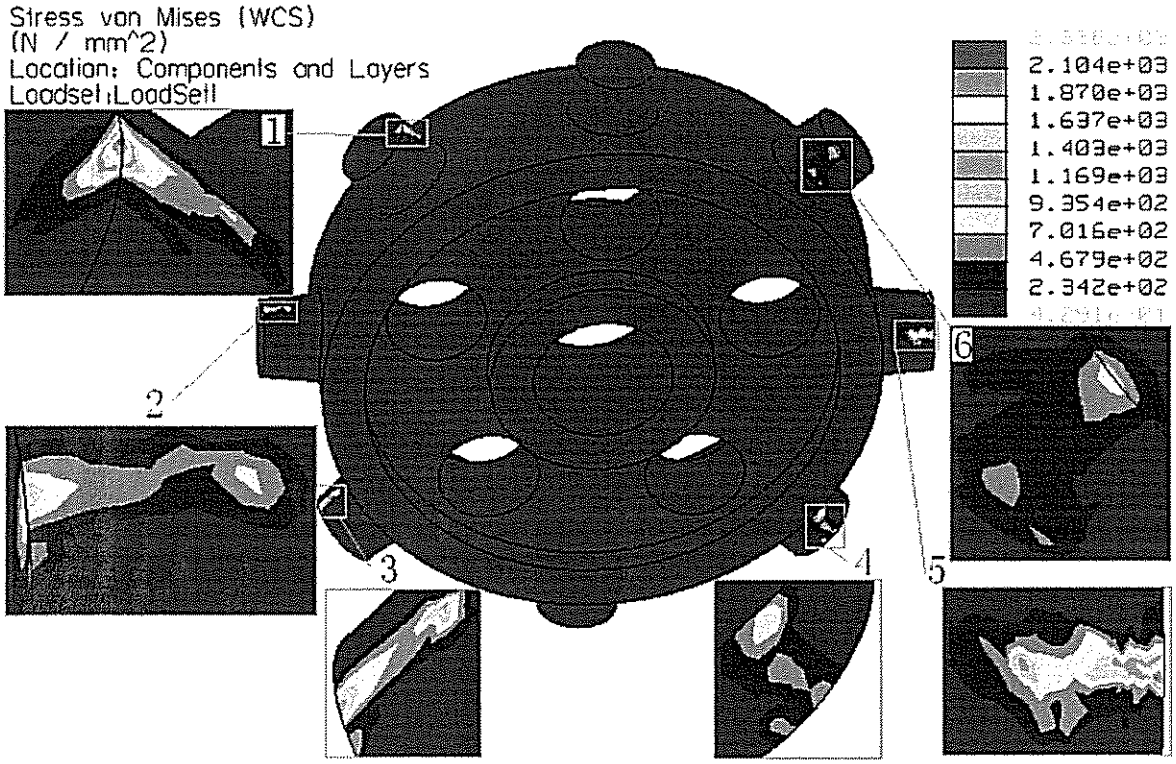

Fig.9 Stress distribution in the planet

5. Changes of the stress distribution

As worm, planet and rotor rotate the stress distribution in the toroidal drive changes. Here, take the stress distribution in the stator as example to illustrate the changes. Changes of the stress distribution in the stator along with planet rotating angle are shown in Fig.10. The stress distribution in the stator at rotating angle $\varphi_1 = 22.5^\circ$ of the planet is shown in Fig.11. From Figs.10 and 11, it is known:

(1) As planet rotates, stress distribution in the stator changes. Hence, the value and position of the maximum stress in the stator change periodically with rotating angle φ_1 of the planet. The time periodic is decided by tooth distance angle $\varphi_0 = 360^0/z_1$ (here, $z_1 = 8$ and $\varphi_0 = 45^\circ$).

(2) Under facewidth angle of the stator $\varphi_v = 120^0$, at angles $[15^0, 30^0]$, the maximum stress in the stator is larger than those at other angles. It is because tooth pair number in contact is two at angles $[15^0, 30^0]$, and tooth pair number in contact is three at other angles. In Fig.10, the maximum stress in the stator is 1978 MPa which is larger than that under three tooth pair contacts. It can be explained as below:

Under facewidth angle of the stator $\varphi_v = 120^0$ and the planet tooth number $z_1 = 8$, tooth pair number in mesh between planet and stator is variable. The changing period is $2\pi/z_1$. The changes of the tooth pair number in mesh is below:

When rotating angle of the planet equals $[0^0, 15^0]$, the tooth pair number in mesh is three.
When rotating angle of the planet equals $[15^0, 30^0]$, the tooth pair number in mesh is two.
When rotating angle of the planet equals $[30^0, 45^0]$, the tooth pair number in mesh is three.
Hence, at angles $[15^0, 30^0]$, each planet tooth carries larger load than that at other angles.

(3) At two tooth pair contact zone, the stress distribution on the stator is still comparatively uniform. In Fig.10 the maximum stress on number 1 tooth is near the maximum stress on number 2 tooth.
(4) For the worm teeth, similar changes of the stress distribution occur (It is not presented here).
(5) Among two teeth mesh zone, the maximum stress changes with rotating angle of the planet. It is because distances between fixed axis and the acting points of the forces changes with the rotating angle of the planet.
(6) Among three teeth mesh zone, the maximum stress changes with rotating angle of the planet as well. It is because the same reason as above.

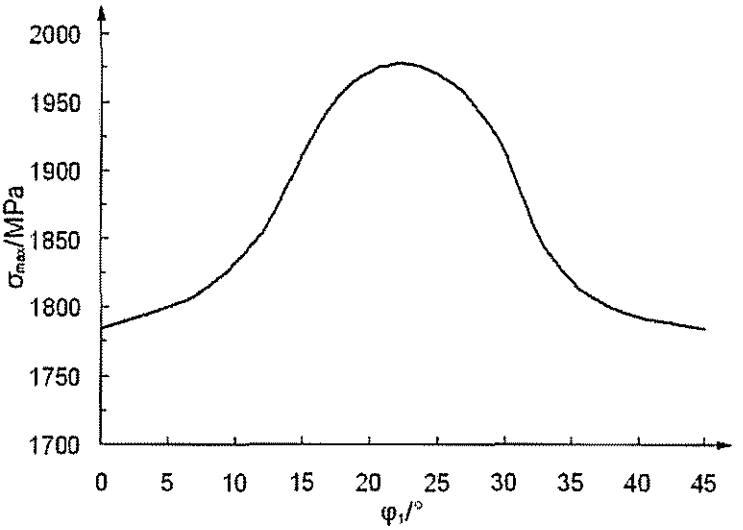

Fig.10 Changes of the maximum stress

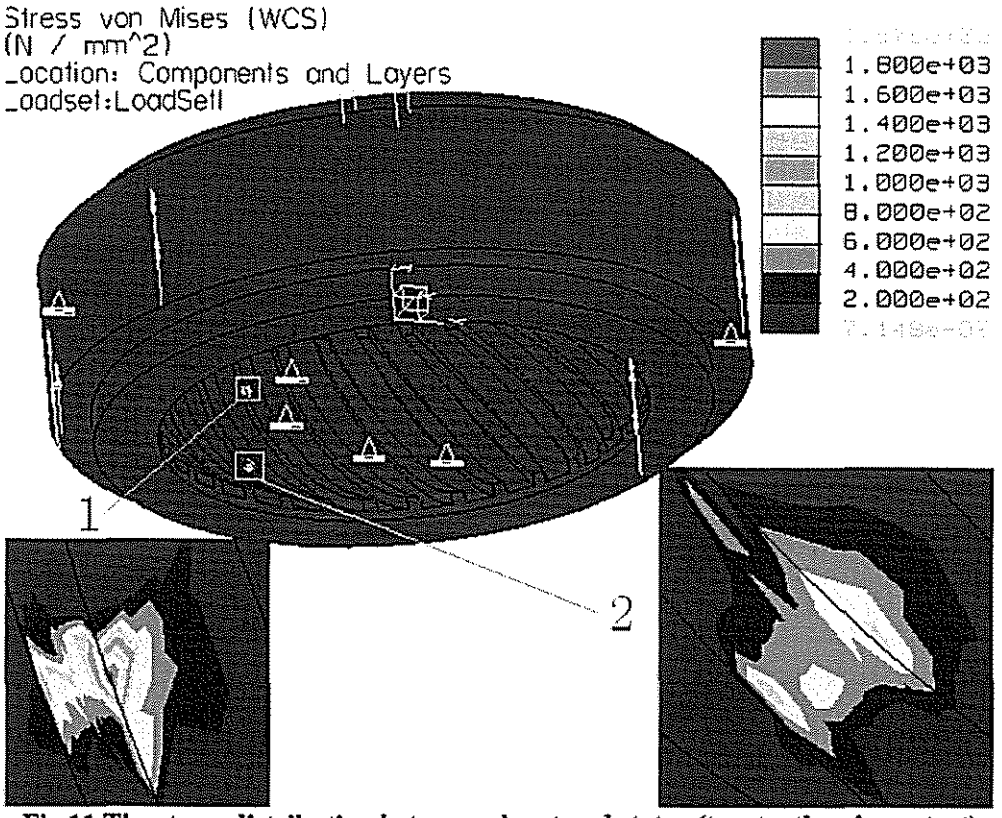

Fig.11 The stress distribution between planet and stator (two tooth pair contact)

Aforementioned results are obtained under condition that only one planet is used. If the planet number is increased, the load can be shared by more planets and more mesh points. In the toroidal drive, up to 12 planets can be grouped around the worm, all of which simultaneously mesh with the worm and the stator to share the load. Therefore, the stress in the drive will be reduced obviously, and much larger load carrying ability can be given by the drive. When planet number equals two, the stress distribution on the stator is shown in Fig.12. From Fig. 12, it is known:

(1) Compared with the drive with one planet, the stress distribution on the stator is similar, but the stress on the stator decreases obviously. Here, the maximum stress in the stator is 1367 MPa.

(2) For the drive with two planets, when rotating angle of the first planet equals zero degree, the number of the meshing tooth pair between the planet and the stator is three, and the number of the meshing tooth pair between another planet and the stator is two. However, the load share between the two planets is comparatively uniform. The maximum stress on the first planet occurs at number 2 tooth, and the maximum stress on the second planet occurs at number 4 tooth. The two maximum stresses are about equal each other.

(3) The utilization of the second planet not only increases sharing points of the load but also improves symmetry of the whole drive system. The symmetry can reduce deformation and displacements of the worm and planets. It causes uniform stress distribution and decrease of the stress.

(4) As planet number further increases the stress in the toroidal drive will decrease further. However, it is necessary to assure alignment accuracy of the planets. Therefore, high alignment accuracy should be assured in order to obtain high load-carrying ability.

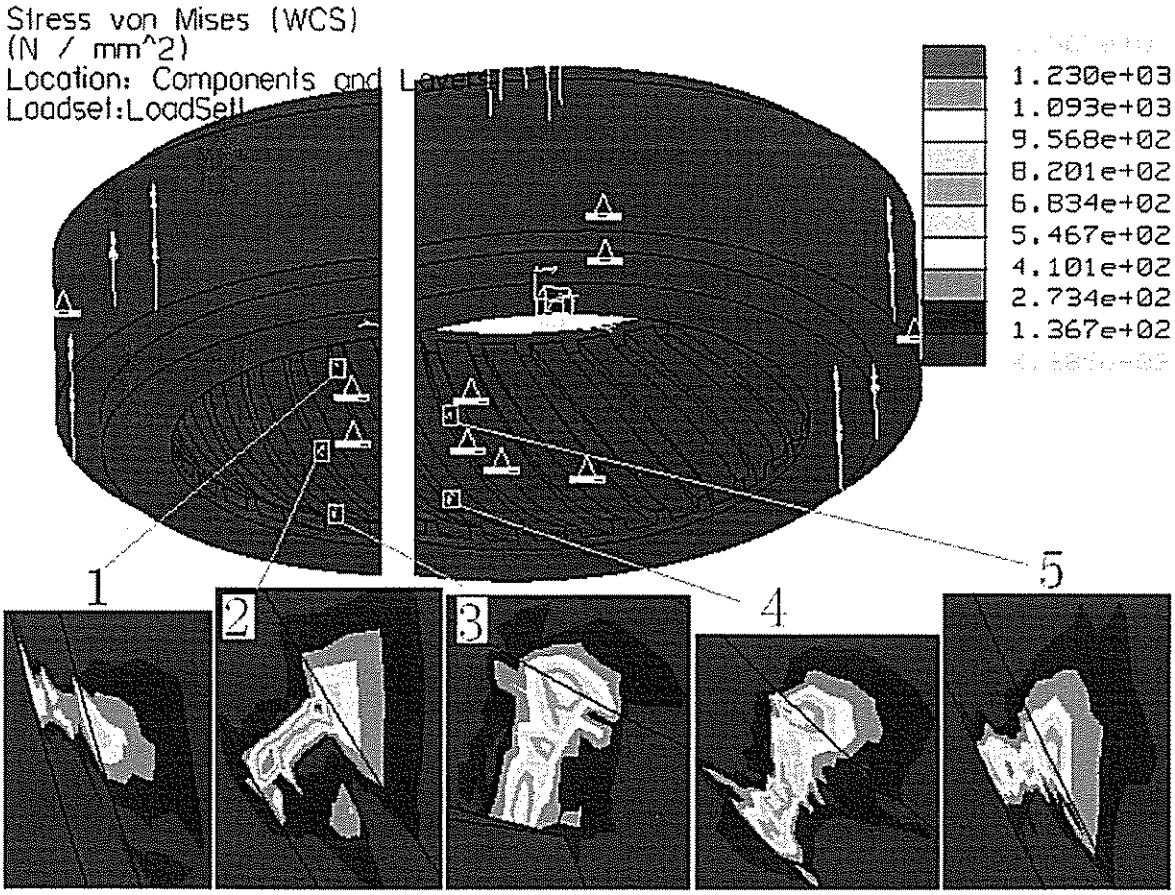

Fig.12 Stress distribution in the stator for two planet toroidal drive

6. Conclusions

In this paper, based on center curve of the teeth, in the environment of the Pro/Engineer software package, the 3D stator and worm models can be constructed, and the 3D model of the drive is constructed as well. FEM analysis package, Pro/Engineer, is used to calculate stress distribution in the elements for the toroidal drive under loads. The stress distributions on worm, stator and planet for the drive are obtained. Changes of the stress distribution along with planet rotating angle and planet number are presented. The main results are:

(1) The load share among the contact tooth pairs is not uniform. Near torque input end, the stress in the worm is the maximum, and near torque output end, the stress in the stator is larger.

(2) For each contact tooth pair, the shape of the contact zone is narrow and long. At the two ends of each contact zone, the stress is larger and dumbbell-shaped stress distribution occurs.

(3) The maximum stress in the stator is larger than that in the worm.

(4) As planet rotates, stress distribution in the stator or worm changes periodically. At two teeth mesh zone, the maximum stress in the stator or worm is larger than those at three teeth mesh zone.

(5) Increase of the planet number can reduce stress in the toroidal drive. It is because uniform stress distribution and more sharing points of the load.

The research is useful in design and manufacture of the drive and can also offer reference for the stress analysis of other drives and structures with toroidal elements.

References.

1. M.R.Kuehnle. Toroidgetriebe.Urkunde uber die Erteilung des deutschen Patents, 1966,1301682.
2. M.R.Kuehnle, H.Peeken, C.Troeder, and S.Cerniak. The Toroidal drive. Mechanical Engineering. 1981, 32(2):32-39.
3. S.Cienriak, W.Clahsen, and A.Laschet. Schlagzahnfrasen von Toroidgetriebe-Statoren. Wt-z. Ind. Fertig. 1983, 73(2):63-66.
4. H.Peeken, S.Cierniak, and Chr.Troeder. Walzfestigkeiten moderner Werkstoffe der Walzpaarung-KugelKugellaufrinne. Konstruktion. 1980, 32(3):89-95.
5. H.Peeken, Chr.Troeder, and K.H.Tooten. Berechnung und Messung der Lastverteilung im Toroidgeriebe. Konstruktion. 1984, 36(3):81-86.
6. K.H.Tooten. Optimierung des Kraftubertra-gungsverhaltens in Getrieben mit Walzkontakten. Antriebstechnik. 1985, 24(7):49-55.
7. Lizhong Xu, Zhen Huang. Contact Stresses for Toroidal drive. Journal of Mechanical Design.Transactions of the ASME. 2003, 125(3): 165-168.
8. Lizhong Xu, Zhen Huang. Mesh Theory for Toroidal drive. Journal of Mechanical Design.Transactions of the ASME.2004,126(3):551-557.